

# New white dwarf and subdwarf stars in the Sloan Digital Sky Survey Data Release 12

S. O. Kepler<sup>1\*</sup>, I. Pelisoli<sup>1</sup>, D. Koester<sup>2</sup>, G. Ourique<sup>1</sup>, A. D. Romero<sup>1</sup>,  
N. Reindl<sup>3</sup>, S. J. Kleinman<sup>4</sup>, D. J. Eisenstein<sup>5</sup>, A. D. M. Valois<sup>1</sup>, L. A. Amaral<sup>1</sup>

<sup>1</sup>*Instituto de Física, Universidade Federal do Rio Grande do Sul, 91501-900 Porto-Alegre, RS, Brazil*

<sup>2</sup>*Institut für Theoretische Physik und Astrophysik, Universität Kiel, 24098 Kiel, Germany*

<sup>3</sup>*Institute for Astronomy and Astrophysics, Kepler Center for Astro and Particle Physics, Eberhard Karls University, Sand 1, 72076, Tübingen, Germany*

<sup>4</sup>*Gemini Observatory, Hilo, Hawaii, 96720, USA*

<sup>5</sup>*Harvard Smithsonian Center for Astrophysics, 60 Garden St., MS #20, Cambridge, MA 02138, USA*

Accepted 2015 October 27. Received 2015 October 26; in original form 2015 August 2

## ABSTRACT

We report the discovery of 6 576 new spectroscopically confirmed white dwarf and subdwarf stars in the Sloan Digital Sky Survey Data Release 12. We obtain  $T_{\text{eff}}$ ,  $\log g$  and mass for hydrogen atmosphere white dwarf stars (DAs) and helium atmosphere white dwarf stars (DBs), estimate the calcium/helium abundances for the white dwarf stars with metallic lines (DZs) and carbon/helium for carbon dominated spectra DQs. We found one central star of a planetary nebula, one ultra-compact helium binary (AM CVn), one oxygen line dominated white dwarf, 15 hot DO/PG1159s, 12 new cataclysmic variables, 36 magnetic white dwarf stars, 54 DQs, 115 helium dominated white dwarfs, 148 white dwarf+main sequence star binaries, 236 metal polluted white dwarfs, 300 continuum spectra DCs, 230 hot subdwarfs, 2 936 new hydrogen dominated white dwarf stars, and 2 675 cool hydrogen dominated subdwarf stars. We calculate the mass distribution of all 5883 DAs with  $S/N \geq 15$  in DR12, including the ones in DR7 and DR10, with an average  $S/N=26$ , corrected to the 3D convection scale, and also the distribution after correcting for the observed volume, using  $1/V_{\text{max}}$ .

**Key words:** white dwarfs – subdwarfs – catalogues – stars: magnetic field

## 1 INTRODUCTION

White dwarf stars are the end product of evolution of all stars with progenitor masses below 7–10.6  $M_{\odot}$ , depending on metallicity (e.g. Ibeling & Heger 2013; Doherty et al. 2015; Woosley & Heger 2015), which corresponds to over 97% of the total number of stars. Most white dwarfs do not generate energy from nuclear fusion, but radiate due to residual gravitational contraction. Because of the degenerate equation of state, this is accompanied by a loss of thermal energy instead of increase as in the case of ideal gases; the evolution of white dwarfs is therefore often simply described as cooling. The radius of a white dwarf star is of the same order of the Earth’s radius, which implies that they have small surface area, resulting in very large cooling times (it takes approximately  $10^{10}$  years for the effective temperature of a normal mass white dwarf to decrease from

100 000 K to near 5 000 K). Consequently, the cool ones are among the oldest objects in the Galaxy. Therefore, studying white dwarfs is extremely important to comprehend the processes of stellar formation and evolution in the Milky Way (e.g. Winget et al. 1987; Bergeron, Saffer, & Liebert 1992; Liebert, Bergeron, & Holberg 2005; Moehler & Bono 2008; Tremblay et al. 2014).

The number of known white dwarf stars is increasing fast thanks to the Sloan Digital Sky Survey (SDSS). The first full white dwarf catalogue from SDSS data (Kleinman et al. 2004) was based on SDSS Data Release 1 (DR1, Abazajian et al. 2003). Using data from the SDSS Data Release 4 (DR4, Adelman-McCarthy et al. 2006), Eisenstein et al. (2006) roughly doubled the number of spectroscopically confirmed white dwarf stars. In the white dwarf catalogue based on the SDSS Data Release 7 (DR7, Abazajian et al. 2009), Kleinman et al. (2013) increased the total number of white dwarf stars by more than a factor of two compared to the catalogue based on DR4 data. They

\* kepler@if.ufrgs.br

**Table 1.** Number of objects and the main classifications in the previous white dwarf catalogues published based on SDSS data releases.

Catalogue	Objects	Main classifications
DR1 <sup>a</sup>	2 551 WDs 240 sds	1 888 DA 171 DB
DR4 <sup>b</sup>	9 316 WDs 928 sds	8 000 DA 731 DB
DR7 <sup>c</sup>	19 713 WDs	12 831 DA 922 DB
DR10 <sup>d</sup>	8 441 WDs 647 sds	6 887 DA 450 DB

<sup>a</sup>Kleinman et al. (2004). <sup>b</sup>Eisenstein et al. (2006).

<sup>c</sup>Kleinman et al. (2013), includes the (re)analysis of stars from previous releases, but does not include subdwarfs..

<sup>d</sup>Kepler et al. (2015).

also (re)analysed all stars from previous releases. Over 8 000 new spectroscopically confirmed white dwarf stars were reported by Kepler et al. (2015) in the analysis of SDSS Data Release 10 (DR10, Ahn et al. 2014). They also improved the candidate selection compared to previous catalogues, implementing an automated search algorithm to search objects which were missed by the other selection criteria. It was also the first white dwarf catalogue based on SDSS data to fit not only DA and DB stars, but also DZ, DQ, and DA+MS pairs. We continue such detailed analysis here with SDSS Data Release 12 (DR12, Alam et al. 2015). More details concerning the previous catalogues are presented in Table 1.

Although the SDSS increased the number of spectroscopically-confirmed white dwarf stars more than an order of magnitude prior to the SDSS, the SDSS sample is far from complete. Target selection considerations of the original SDSS (up to DR8) implied that white dwarf selection for spectroscopy was incomplete (e.g. Gentile Fusillo, Gänsicke, & Greiss 2015). In the SDSS DR12, the ancillary target programme 42 (Dawson et al. 2013) obtained the spectra of an additional 762 colour selected white dwarf candidates that were missed by prior SDSS spectroscopic surveys, i.e., up to DR10. Here, we report on our search for new white dwarfs from the SDSS Data Release 12 (Alam et al. 2015), which in total observed photometrically one third of the celestial sphere and obtained 4.3 million useful optical spectra. Our catalogue does not include stars reported in the earlier catalogues, except for classification corrections.

## 2 TARGET SELECTION

Even though targeting in SDSS produced the largest spectroscopic sample of white dwarfs, much of SDSS I and II white dwarf targeting required that the objects be unblended, which caused many bright white dwarfs to be skipped (for a detailed discussion, see Section 5.6 of Eisenstein et al. 2006). The BOSS ancillary targeting programme (Dawson et al. 2013) relaxed this requirement and imposed colour cuts to focus on warm and hot white dwarfs. Im-

portantly, the BOSS spectral range extends further into the UV, covering from 3 610 Å to 10 140 Å, with spectral resolution 1560-2270 in the blue channel, and 1850-2650 in the red channel (Smee et al. 2013), allowing full coverage of the Balmer lines.

The targeted white dwarfs in SDSS-III were required to be point sources with clean photometry, and to have USNO-B Catalog counterparts (Monet et al. 2003). They were also restricted to regions inside the DR7 imaging footprint and required to have colours within the ranges  $g < 19.2$ ,  $(u-r) < 0.4$ ,  $-1 < (u-g) < 0.3$ ,  $-1 < (g-r) < 0.5$ , and to have low Galactic extinction  $A_r < 0.5$  mag. Additionally, targets that did not have  $(u-r) < -0.1$  and  $(g-r) < -0.1$  were required to have USNO proper motions larger than 2 arcsec per century. Objects satisfying the selection criteria that had not been observed previously by the SDSS (ANC 42) were denoted by the WHITEDWARF\_NEW target flag, while those with prior SDSS white dwarf photometric classification (ANC 43) are assigned the WHITEDWARF\_SDSS flag. Some of the latter were re-observed with BOSS in order to obtain the extended wavelength coverage that the BOSS spectrograph offers. The targeting colour selection included DA stars with temperatures above  $\sim 14\,000$  K, helium atmosphere white dwarfs above  $\sim 8\,000$  K, as well as many rarer classes of white dwarfs. Hot subdwarfs (sdB and sdO) were targeted as well.

Our selection of white dwarf candidates among DR12 objects was similar to that reported for DR10 (Kepler et al. 2015). We did not restrict our sample by magnitude, but by  $S/N \geq 3$ . In addition to the 762 targeted white dwarf candidates after DR10 by ANC 42, we selected the spectra of any object classified by the ELODIE pipeline (Bolton et al. 2012) as a white dwarf, which returned 35 708 spectra, an O, B or A star, which returned another 144 471 spectra. Our general colour selection from Kleinman et al. (2013), which takes into account that SDSS multi-colour imaging separates hot white dwarf and subdwarf stars from the bulk of the stellar and quasar loci in colour-colour space (Harris et al. 2003), returned 68 836 new spectra, from which we identified another 2 092 white dwarfs, 79 subdwarfs, 36 cataclysmic variables, and 3 PG 1159. Most of these spectra were overlapping with the ELODIE selections.

We also used an automated search algorithm which assumes that the spectra of two objects with the same composition, effective temperature and surface gravity differ only in flux, due to different distances, and slope, because of reddening and calibration issues. This algorithm determines a polynomial of order between zero and two which minimizes the difference between each spectrum and a sample of models, allowing the determination of the most likely spectral class of each object. Running this search over the whole 4.5 million spectra from DR 12 recovered more than 80% of our sample and found 400 white dwarf stars missed by previous searches.

## 3 DATA ANALYSIS

The data analysed here were reduced by the v5\_0\_7 spectroscopic reduction pipeline of Bolton et al. (2012). After visual identification of the spectra as a probable white dwarf, we fitted the optical spectra to DA and DB local thermody-

namic equilibrium (LTE) grids of synthetic non-magnetic spectra derived from model atmospheres (Koester 2010). The DA model grid uses the  $ML2/\alpha = 0.6$  approximation, and for the DBs we use the  $ML2/\alpha = 1.25$  approximation, to be consistent with Kleinman et al. (2013) and Kepler et al. (2015). Our DA grid extends up to  $T_{\text{eff}} = 100\,000$  K, but NLTE effects are not included. Napiwotzki (1997) concluded pure hydrogen atmospheres of DA white dwarfs are well represented by LTE calculations for effective temperatures up to 80 000 K, but when traces of helium are present, non-local thermodynamic equilibrium (NLTE) effects on the Balmer lines occur, down to effective temperatures of 40 000 K. Napiwotzki (1997) concluded LTE models should exclude traces of helium for the analysis of DA white dwarfs. We fitted the spectral lines and photometry separately (Koester 2010), selecting between the hot and cool solutions using photometry as an indicator.

Of the 762 objects targeted specifically as new white dwarf spectra by BOSS as Ancillary Programme 42, 19 were not identified as white dwarfs or subdwarfs by us. Of the Ancillary Program 43 of WHITEDWARF\_SDSS already observed, 5 in 80 colour selected stars are in fact quasars. Gentile Fusillo, Gänsicke, & Greiss (2015) reports that only 40% of their SDSS colour selected sample with high probability of being a white dwarf has spectra obtained by SDSS.

The SDSS spectra we classified as white dwarfs or subdwarfs have a g-band signal-to-noise ratio  $85 \geq S/N(g) \geq 3$ , with an average of 12. The lowest S/N in the g-band occurs for stars cooler than 7 000 K, but they have significant S/N in the red part of the spectrum.

We include in our tables the new proper motion determinations of Munn et al. (2014) and use them to separate DCs from BL Lac spectra. We applied complete, consistent human identifications of each candidate white dwarf spectrum.

### 3.1 Spectral Classification

Because we are interested in obtaining accurate mass distributions for our DA and DB stars, we were conservative in labelling a spectrum as a clean DA or DB, adding additional subtypes and uncertainty notations (:) if we saw signs of other elements, companions, or magnetic fields in the spectra. While some of our mixed white dwarf subtypes would probably be identified as clean DAs or DBs with better signal-to-noise spectra, few of our identified clean DAs or DBs would likely be found to have additional spectral features within our detection limit.

We looked for the following features to aid in the classification for each specified white dwarf subtype:

- Balmer lines — normally broad and with a steep Balmer decrement [DA but also DAB, DBA, DZA, and subdwarfs]
- HeI 4471Å [DB, subdwarfs]
- HeII 4686Å [DO, PG1159, sdO]
- C2 Swan band or atomic CI lines [DQ]
- CaII H & K [DZ, DAZ, DBZ]
- CII 4367Å [HotDQ]
- Zeeman splitting [magnetic white dwarfs]
- featureless spectrum with significant proper motion [DC]

**Table 2.** Numbers of newly identified stars by type.

No. of Stars	Type
2 675	sdA
1 964	DA <sup>a</sup>
300	DC
236	DZ
183	sdB
104	WD+MS <sup>b</sup>
66	DB
71	DAZ
54	DQ
47	sdO
27	DBA
28	DAH
14	DO/PG 1159
12	CV
7	DZH
6	DAO
3	DAB
2	DBH
1	DBZ
1	Dox
1	AM CVn (SDSS J131954.47+591514.84)
1	CSPN (SDSS J141621.94+135224.2)

<sup>a</sup>Pure and certain DAs. <sup>b</sup>These spectra show both a white dwarf star and a companion, non-white dwarf spectrum, usually a main sequence M star.

- flux increasing in the red [binary, most probably M companion]
- OI 6158Å [Dox]

We also found 8 of stars to have an extremely steep Balmer decrement (i.e. only a broad H $\alpha$  and sometimes H $\beta$  is observed while the other lines are absent) that could not be fit with a pure hydrogen grid, or indicated extremely high gravities. We find that these objects are best explained as helium-rich DAs, and denote them DA-He.

We finally note that the white dwarf colour space also contains many hot subdwarfs. It is difficult to distinguish a low mass white dwarf from a subdwarf, as they are both dominated by hydrogen lines and the small differences in surface gravity cannot be spotted by visual inspection alone. We therefore extended the model grid to  $\log g = 5.00$  for  $T_{\text{eff}} \geq 25\,000$  K, and  $\log g = 3.75$  for  $T_{\text{eff}} < 25\,000$  K, to separate white dwarfs ( $\log g \geq 6.5$ ), subdwarfs ( $6.5 > \log g \geq 5.5$ ) and main sequence stars ( $\log g \leq 4.75$ ) (see section 4.1 and 4.7), but we caution that the differences in the line widths for DAs cooler than  $\simeq 8000$  K and hotter than  $\simeq 30\,000$  K are minor, with changing gravity. We use sdA to denote spectra with  $6.5 > \log g \geq 5.5$  and  $T_{\text{eff}} \leq 20\,000$  K. Table 2 lists the number of each type of white dwarf and subdwarf stars we identified.

As an independent check, and to be consistent with the earlier SDSS white catalogues, we also fitted all DA and DB white dwarf spectra and colours with the AUTOFIT code described in Kleinman et al. (2004), Eisenstein et al. (2006) and Kleinman et al. (2013). AUTOFIT fits only clean DA and DB models. In addition to the best fitting model parameters, it also outputs flags for other features noted in the spectrum, like a possible dM companion. These fits include SDSS imaging photometry and allow for reflusing of the models by a low-order polynomial to incorporate effects

of unknown reddening and spectrophotometric flux calibration errors.

## 4 RESULTS

### 4.1 Masses

Kleinman et al. (2013) limited the white dwarf classification to surface gravity  $\log g \geq 6.5$ . At the cool end of our sample,  $\log g = 6.5$  corresponds to a mass around  $0.2 M_{\odot}$ , well below the single mass evolution in the lifetime of the Universe. The He-core white dwarf stars in the mass range  $0.2 - 0.45 M_{\odot}$ , referred to as low-mass white dwarfs, are usually found in close binaries, often double degenerate systems (Marsh, Dhillon & Duck 1995), being most likely a product of interacting binary stars evolution. More than 70% of those studied by Kilic et al. (2011) with masses below  $0.45 M_{\odot}$  and all but a few with masses below  $0.3 M_{\odot}$  show velocity variations (Brown et al. 2013; Gianninas et al. 2014). Kilic, Stanek & Pinsonneault (2007) suggests single low-mass white dwarfs result from the evolution of old metal-rich stars that truncate evolution before the helium flash due to severe mass loss. They also conclude all white dwarfs with masses below  $\simeq 0.3 M_{\odot}$  must be a product of binary star evolution involving interaction between the components, otherwise the lifetime of the progenitor on the main sequence would be larger than the age of the Universe.

DA white dwarf stars with masses  $M \leq 0.45 M_{\odot}$  and  $T_{\text{eff}} < 20\,000$  K are Low Mass and Extremely Low Mass (ELM) as found by Brown et al. (2010), Kilic et al. (2011), Kilic et al. (2012), Brown et al. (2012), Brown et al. (2013), and Gianninas et al. (2014). Hermes et al. (2012), Hermes et al. (2013a), Hermes et al. (2013b), and Bell et al. (2015) found pulsations in six of these ELMs, similar to the pulsations seen in DAVs (ZZ Ceti stars), as described in Van Grootel et al. (2013). Maxted et al. (2014) found 17 pre-ELMs, i.e., helium white dwarf precursors, and Maxted et al. (2014) report pulsations in one of them. Pulsations are an important tool to study the stellar interior, and Córscico & Althaus (2014a), Córscico & Althaus (2014b), Córscico & Althaus (2015), Istrate et al. (2014a), and Istrate (2015) report on theoretical models and pulsations of ELMs.

We classified as DAs those with  $\log g \geq 6.5$  as in Kleinman et al. (2013), and sdAs those with  $6.5 > \log g \geq 5.5$  when  $T_{\text{eff}} \leq 20\,000$  K (see section 4.7). Low metallicity main sequence stars have an upper limit to  $\log g \lesssim 4.75$ . To select the low  $\log g$  limit, we use an external, systematic uncertainty in our surface gravity determinations of  $3\sigma(\log g) = 3 \times 0.25$ , around  $15 \times$  our average internal fitting uncertainty.

Fig. 1 shows surface gravity,  $\log g$ , as a function of the effective temperature  $T_{\text{eff}}$ , estimated for all 5884 DAs spectroscopically identified in DR7 to DR12 with SDSS spectral  $S/N \geq 15$ . We include corrections to  $T_{\text{eff}}$  and  $\log g$  based on three-dimensional convection calculations from Tremblay et al. (2013).

We use the mass–radius relations of Renedo et al. (2010) and Romero, Campos, & Kepler (2015) for carbon–oxygen DA white dwarfs with solar metallicities to calculate the mass of our identified DA stars from the  $T_{\text{eff}}$  and  $\log g$  values obtained from our fits, after correcting to 3D convec-

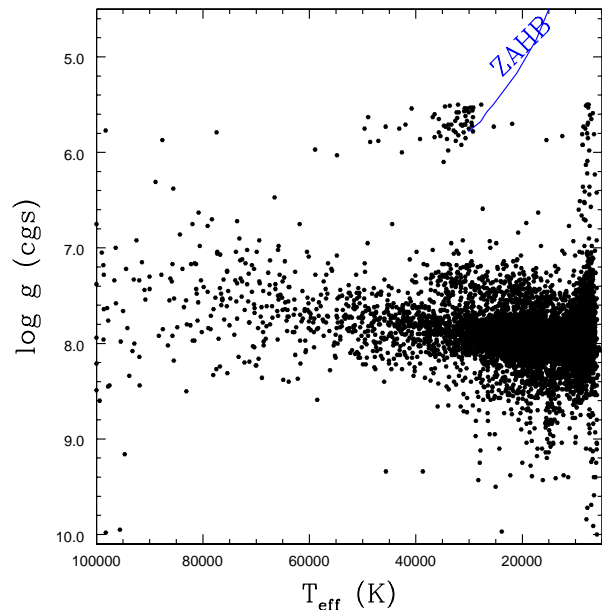


**Figure 1.** Surface gravity ( $\log g$ ) and effective temperature ( $T_{\text{eff}}$ ) estimated for all DA white dwarf stars in DR7 to DR12 with spectral  $S/N_g \geq 15$ , after applying three-dimensional convection atmospheric model corrections from Tremblay et al. (2013). The Zero Age Horizontal Branch (ZAHB) plotted was calculated with solar composition models. It indicates the highest possible surface gravity for a hot subdwarf. Stars with  $T_{\text{eff}} \leq 45\,000$  K and smaller surface gravities than the ZAHB are sdBs.

tion. These mass–radius relations are based on full evolutionary calculations appropriate for the study of hydrogen-rich DA white dwarfs that take into account the whole evolution of progenitor stars. The sequences are computed from the zero-age main sequence, through the hydrogen and helium central burning stages, thermal pulsations and mass-loss in the asymptotic giant branch phase and finally the planetary nebula domain. The white dwarf masses for the resulting sequences range from  $0.525$  to  $1.024 M_{\odot}$ , covering the stellar mass range for C–O core DAs. For high-gravity white dwarf stars, we used the mass–radius relations for O–Ne core white dwarfs given in Althaus et al. (2005) in the mass range from  $1.06$  to  $1.30 M_{\odot}$  with a step of  $0.02 M_{\odot}$ . For the low-gravity white dwarf and cool subdwarf stars, we used the evolutionary calculations of Althaus, Miller Bertolami, & Córscico (2013) for helium-core white dwarfs with stellar mass between  $0.155$  to  $0.435 M_{\odot}$ , supplemented by sequences of  $0.452$  and  $0.521 M_{\odot}$  calculated in Althaus et al. (2009a).

The spectra we classified as DBs belong to 116 stars. 27 of these are DBAs, one is a DBZ (SDSS J122649.96+444513.59), and 8 are DB+M. To calculate the DB white dwarf masses in the catalogue, we relied on the evolutionary calculations of hydrogen-deficient white dwarf stars with stellar masses between  $0.515$  and  $0.870 M_{\odot}$  computed by Althaus et al. (2009b). These sequences have been derived from the born-again episode responsible for the hydrogen deficient white dwarfs. For high- and low-gravity DBs, we used the same O–Ne and helium evolutionary sequences described before.

S/N <sub>g</sub>	N	$\langle M_{\text{DA}} \rangle$ ( $M_{\odot}$ )
15	5884	$0.608 \pm 0.002$
25	2591	$0.620 \pm 0.002$
50	265	$0.644 \pm 0.008$

**Table 3.** Mean masses for all DAs, corrected to 3D convection.

To calculate a reliable mass distribution for DAs, we selected only the  $S/N \geq 15$  spectra with temperatures well fit by our models. Including the DAs from DR7 (Kleinman et al. 2013) and DR10 (Kepler et al. 2015), we classified a total of 5884 spectra as clean DAs with  $S/N \geq 15$ , with a mean  $S/N = 26 \pm 11$ . Table 3 presents the mean masses for different signal-to-noise limits. Gianninas, Bergeron, & Fontaine (2005) estimate the increase of the uncertainty in the surface gravity from  $\Delta \log g \simeq 0.06$  dex to  $\Delta \log g \simeq 0.25$  dex when the  $S/N$  decreases from 50 to 15. Genest-Beaulieu & Bergeron (2014) conclude there appears to be a small residual zero point offset in the absolute fluxes of SDSS spectra. If the differences in the mean masses with  $S/N$  are not due to systematic (not random) effects, it could be the reflection of different populations, as faint stars perpendicular to the disk of the Galaxy could have different metallicities, and therefore different star formation mass functions and different Initial-to-Final-Mass relations (Romero, Campos, & Kepler 2015).

The mean masses estimated in our DR7 to DR12 sample are smaller than those obtained by Kepler et al. (2015), even with the use of the 3D corrections for the whole sample.

Fig. 2 shows the mass histogram for the 5884 DAs with  $S/N \geq 15$  and Fig. 3 shows the mass distribution after correcting by the observed volume, following Schmidt (1968, 1975), Green (1980), Stobie, Ishida, & Peacock (1989), Liebert, Bergeron, & Holberg (2003), Kepler et al. (2007), Limoges & Bergeron (2010) and Rebassa-Mansergas et al. (2015). This correction takes into account the shape of the galactic disk, assuming a scale height of 250 pc, minimum ( $g \simeq 14.5$ ) and maximum ( $g = 19$ ) magnitudes, for a complete sample. Green (1980) propose completeness can be estimated from  $\langle V/V_{\text{max}} \rangle$ , which is equal to 0.48 in our sample, close to the expected value of 0.50.

Rebassa-Mansergas et al. (2015) limit their sample to bolometric magnitude  $M_{\text{bol}} \leq 13$ , because Gentile Fusillo, Gänsicke, & Greiss (2015) estimates completeness of 40% down to this magnitude. Such bolometric magnitude corresponds to  $T_{\text{eff}} \gtrsim 8500$  K around masses  $0.6 M_{\odot}$ , and to  $T_{\text{eff}} \gtrsim 10000$  K around masses  $1.0 M_{\odot}$ . We do not limit our sample to  $M_{\text{bol}} \leq 13$ . We find 94 DA white dwarf stars with masses above  $1.0 M_{\odot}$  and  $S/N \geq 15$ , and applying the volume correction to them, find a lower limit to their density of  $0.000026 M_{\odot} \text{ pc}^{-3}$ . 20 of these have  $M_{\text{bol}} > 13$ . We did not apply any completeness correction by proper motion (e.g. Lam, Rowell, & Hambly 2015) because we did not apply a consistent limit on the proper motion. The distribution for masses above the main peak around  $0.6 M_{\odot}$  is significantly uneven, possibly the outcome of distinct formation mechanisms, including single star formation, accretion and mergers.

The DB mass distribution obtained from models including hydrogen contamination, is discussed in Koester & Kepler (2015). **As our temperatures and sur-**

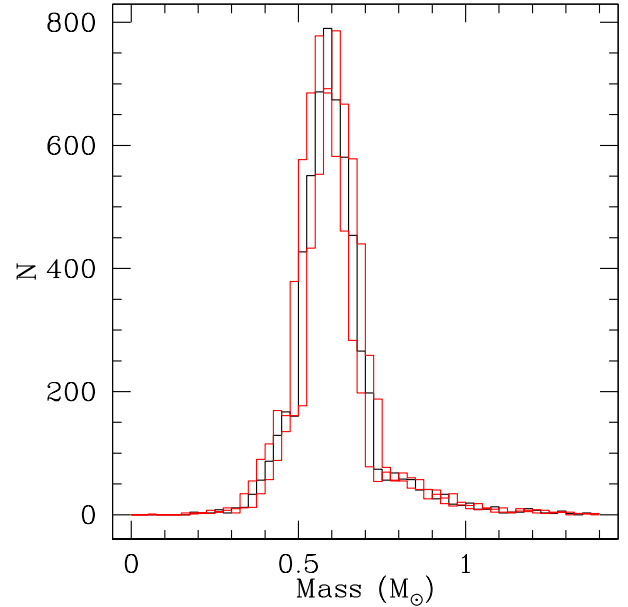


**Figure 2.** Histogram for the mass distribution of 5884  $S/N \geq 15$  DAs versus mass, for  $\log g$  corrected to three-dimensional convection models using the corrections reported in Tremblay et al. (2013). The colored lines show the  $-1\sigma$  and  $+1\sigma$  uncertainties.

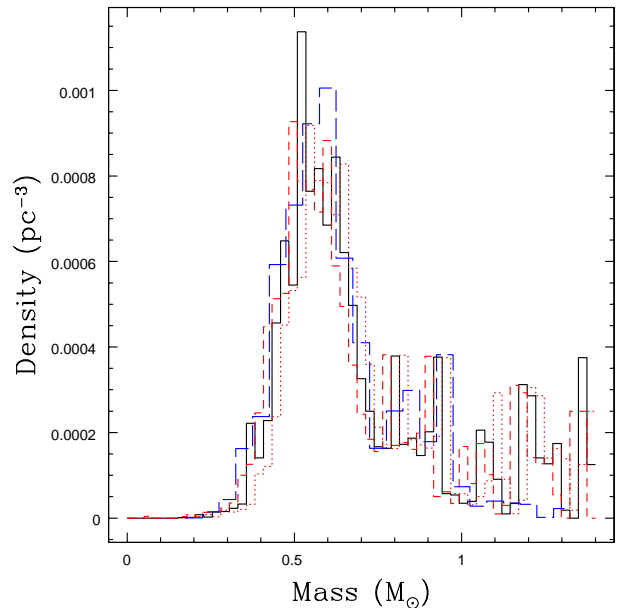


**Figure 3.** Histogram for the density distribution of  $S/N \geq 15$  DAs versus mass, for  $\log g$  corrected to three-dimensional convection models, after correcting by the observed volume and by 40% completeness from Gentile Fusillo, Gänsicke, & Greiss (2015). The colored lines show the  $-1\sigma$  and  $+1\sigma$  uncertainties. The long dashed (blue) histogram is the one from Rebassa-Mansergas et al. (2015), limited to  $M_{\text{bol}} > 13$ .

**Table 4.** Magnetic field for DZHs

SDSS J	Plate-MJD-Fiber	B (MG)	$\sigma(B)$ (MG)
003708.42-052532.80	7039-56572-0140	7.2	0.2
010728.47+265019.94	6255-56240-0896	3.4	0.1
110644.27+673708.64	7111-56741-0676	3.3	0.1
111330.27+275131.41	6435-56341-0036	3.0	0.1
114333.46+661532.01	7114-56748-0973	9.0	1.5
225448.83+303107.15	6507-56478-0276	2.5	0.1
233056.81+295652.68	6501-56563-0406	3.4	0.3

face gravities were estimated with pure DB models, while those of [Koester & Kepler \(2015\)](#) include Hydrogen contamination, their values are more accurate.

#### 4.2 Magnetic Fields and Zeeman Splittings

When examining each white dwarf candidate spectrum by eye, we found 36 stars with Zeeman splittings indicating magnetic fields above 2 MG — the limit where the line splitting becomes too small to be identified at the SDSS spectral resolution. This number is similar to our findings reported for DR7 in [Kepler et al. \(2013\)](#) and DR10 ([Kepler et al. 2015](#)).

If the line splitting and magnetic fields were not recognized, the spectral fittings of DA and DB models would have rendered too high  $\log g$  determinations due to magnetic broadening being misinterpreted as pressure broadening.

We also identified seven cool DZH (Table 4), similar to those identified by [Hollands, Gänsicke, & Koester \(2015\)](#).

We estimated the mean fields for the new DAHs following [Külebi et al. \(2009\)](#) as being from 3 MG to 80 MG. We caution that stars with large fields are difficult to identify because fields above around 30 MG, depending on effective temperature and signal-to-noise, intermixes subcomponents between different hydrogen series components so much that it becomes difficult to identify the star as containing hydrogen at all, and affect the colours significantly. Additionally white dwarf stars with fields above 100 MG (see Fig. 4) represent the intermediate regime in which the spectra have very few features, except for a few stationary transitions that have similar wavelengths for a reasonable distribution of magnetic fields over the surface of the star.

In [Kleinman et al. \(2013\)](#) and [Kepler et al. \(2013\)](#), we mis-classified SDSS J110539.77+250628.6, Plate-MJD-Fiber (P-M-F)=2212-53789-0201 and SDSS J154012.08+290828.7, P-M-F=4722-55735-0206 as magnetic, but they are in fact CVs. SDSS J110539.77+250628.6 was identified as an AM Her star by [Liu et al. \(2012\)](#). Here, we update the identification of SDSS J154012.08+290828.7 to a cataclysmic variable (CV), with a period around 0.1 d based on data from the Catalina Sky Survey (CSS, [Drake et al. 2009](#)). We found another 14 cataclysmic variables based on seeing hydrogen and/or helium lines in emission. Most are variable in the CSS.

#### 4.3 DCs and BL Lac

Featureless optical spectra are the signature of DC

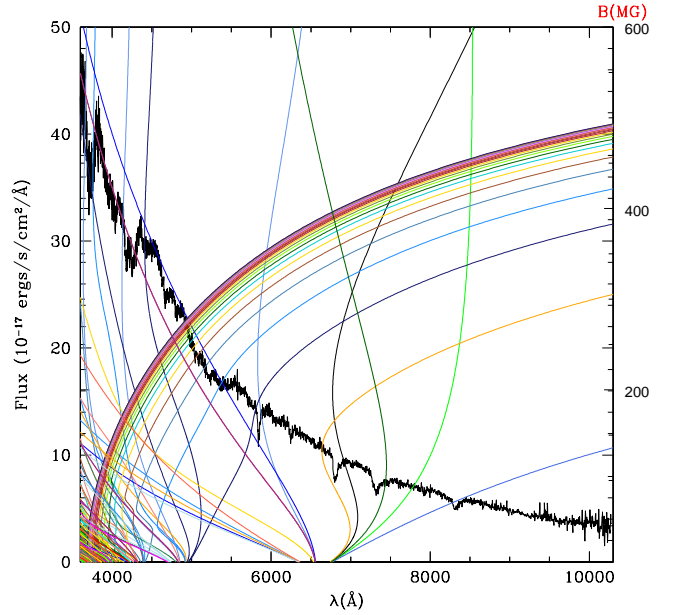


**Figure 4.** Observed spectrum of the DAH, SDSS J112148.77+103934.1 with  $g = 17.98 \pm 0.03$  and  $B \simeq 309$  MG. The coloured lines indicate the positions of each theoretical Zeeman split Balmer line subcomponent, assuming a dipole magnetic field of strength indicated in the right axis. Even low fields produce large splittings of the higher Balmer lines. The theoretical models are from [Schimeczek et al. \(2013\)](#); [Schimeczek & Wunner \(2014a,b\)](#).

white dwarfs, but also from extragalactic BL Lac objects. BL Lac objects are strong sources of radio emission, while non-interacting DCs are not. DCs, if bright enough to be detected in all images, generally have measurable proper motions, as their inherent dimness means they are relatively close to us. To separate DCs from BL Lacs, we searched for 1.4 GHz radio emission in the literature and looked for measured proper motions in [Munn et al. \(2014\)](#). We found 41 of our DC candidates were really BL Lac objects based on detectable radio emission. **We discarded the objects with radio emission, as well as those with no radio emission and no proper motion.**

#### 4.4 DZs

Of the new white dwarfs in our sample, 3% have spectra with metal lines, probably due to accretion of rocky material around the stars (e.g. [Graham et al. 1990](#); [Jura 2003](#); [Koester, Gänsicke, & Farihi 2014](#)). Calcium and magnesium in general have the strongest lines for white dwarfs at these temperatures.

We identified two DBZs as having unusual oxygen lines. SDSS J124231.07+522626.6, P-M-F 6674-56416-0868, with  $T_{\text{eff}} = 13000$  K, was misclassified as an sdB from spectrum P-M-F 0885-52379-0112 in [Eisenstein et al. \(2006\)](#), and identified by us here as an oxygen-rich DBZ, possibly formed by accretion of an water rich asteroid as suggested by [Raddi et al. \(2015\)](#) and [Farihi, Gänsicke, & Koester \(2013\)](#). SDSS J123432.65+560643.1, spectrum P-M-F 6832-56426-0620, was identified as DBZA in [Kleinman et al.](#)

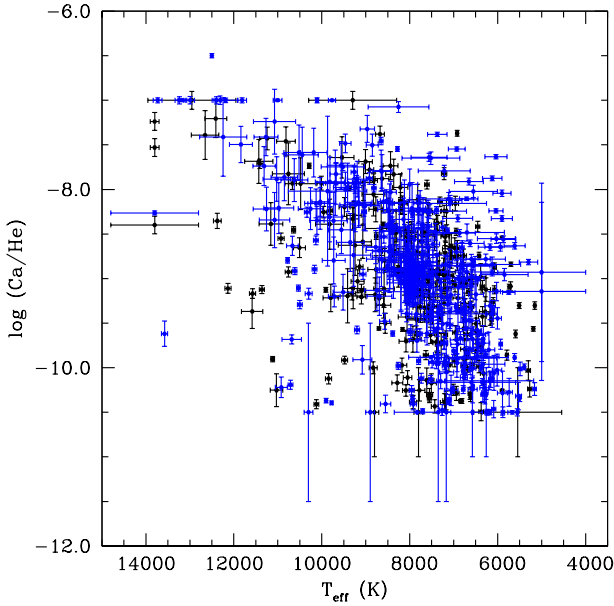


**Figure 5.** Calcium/Helium abundances estimated for DZs contained in DR7 to DR12.

(2013) from P-M-F 1020-52721-0540. but is a DBZ. We estimate  $T_{\text{eff}} = 12\,400 \pm 120$  K,  $\log g = 8.135 \pm 0.065$ .

We fit the spectra of each of the 236 stars classified as DZs to a grid of models with Mg, Ca and Fe ratios equal to the averages from the cool DZs in Koester et al. (2011), and Si added with the same abundance as Mg (Koester, Gänsicke, & Farihi 2014). These models have a fixed surface gravity of  $\log g = 8.0$  as it is not possible to otherwise estimate it from the spectra. The absolute values for  $\log \text{Ca}/\text{He}$  range from -7.25 to -10.50. Fig. 5 shows the calcium/helium abundance for the 246 DZs identified in DR12, in addition to those of DR7 and DR10. There seems to be a decrease of Ca/He abundances at lower temperatures. This trend might be explained if all stars had the same metal-rich material accretion rate, but the material becomes more diluted at cooler temperatures due to the increasing convection layer size.

#### 4.5 DQs

Only 0.7% of the newly identified spectra in our sample are dominated by carbon lines that are believed to be due to dredge-up of carbon from the underlying carbon-oxygen core through the expanding He convection zone (e.g. Koester, Weidemann, & Zeidler 1982; Pelletier et al. 1986; Koester & Knist 2006; Dufour et al. 2007). These stars are in general cooler than  $T_{\text{eff}} = 12\,000$  K.

We fitted the spectra of the stars (classified as cool DQs) to a grid of models reported by Koester & Knist (2006). The models have a fixed surface gravity of  $\log g = 8.0$  as it is not possible to otherwise estimate it from the spectra. The absolute values for  $\log \text{C}/\text{He}$  range from -8 to -4, and effective temperatures vary from 13000 K to 4400 K. Fig. 6 shows the carbon/helium abundance for the 54 new cool DQs identified here in addition to those from DR7 and DR10. There is a decrease of C/He abundances at lower temperatures,

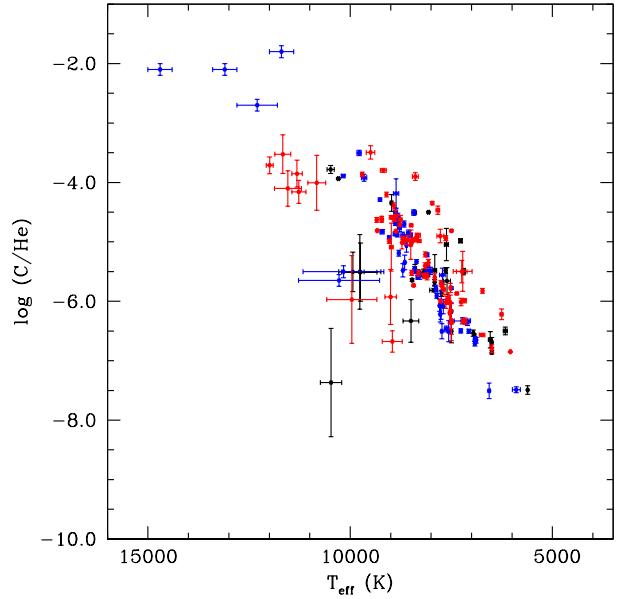


**Figure 6.** Carbon/Helium abundances estimated for DQs. The decrease with decreasing temperature comes from the increase in transparency and deepening convection zone. The darker points are the new DQs from DR12. The lighter (red and blue) points are the results of our fits with the same models for the cool DQs in Kleinman et al. (2013) and Kepler et al. (2015).

probably caused by the deepening of the convection zone, diluting any surface carbon.

#### 4.6 White dwarf-main sequence binaries

We have identified 104 new white dwarfs that are part of apparent binary systems containing main-sequence companions (WD-MS binaries). The majority (96) of our new systems contain a DA white dwarf and a M dwarf secondary star (DA+M).

#### 4.7 Subdwarfs

Hot subdwarfs are core He burning stars. Following Németh, Kawka, & Vennes (2012), Drilling et al. (2013), Nemeth et al. (2014a), and Nemeth et al. (2014b), we have classified stars with  $\log g < 6.5$  and  $45\,000 \text{ K} \geq T_{\text{eff}} \geq 20\,000$  K as subdwarfs: sdOs if He II present and sdBs if not. Nemeth et al. (2014a) and Rauch et al. (2014) discuss how the He abundances typical for sdB stars affect the Non Local Thermodynamical Equilibrium (NLTE) atmosphere structure. To a lower extent, CNO and Fe abundances are also important in deriving accurate temperatures and gravities. Our determinations of  $T_{\text{eff}}$  and  $\log g$  do not include NLTE effects or mixed compositions, so they serve only as a rough estimate. We classified 47 new sdOs and 183 new sdBs.

The Extreme Low Mass white dwarf catalog (Gianninas et al. 2015) lists 73 stars with  $\log g \geq 4.8$ , most with detected radial velocity variations demonstrating they are in binary system. We classified the hydrogen dominated spectra with  $6.5 > \log g_{\text{sDA}} \geq 5.5$  and  $T_{\text{eff}} \leq 20\,000$  K

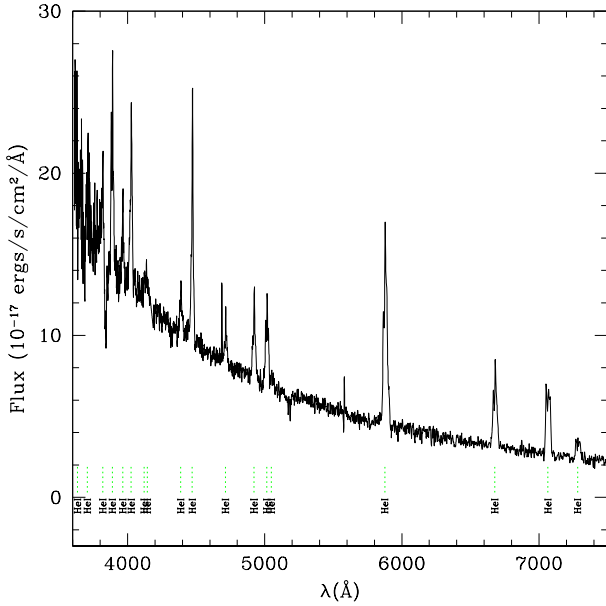


**Figure 7.** Spectra of the AM CVn double degenerate SDSS J131954.47+591514.84 ( $g = 19.106 \pm 0.015$ , proper motion = 33 mas/yr).

as sdAs. These spectra look like main sequence low metallicity A stars, but their estimated surface gravities with  $\log g_{\text{sdA}} \geq 5.5$  are at least  $3\sigma$  (external) larger than those of main sequence stars  $\log g_{\text{MS}} < 4.75$  (Heiter et al. 2015). We caution that the spectral lines and colours used in our analysis are weakly dependent on surface gravity for  $T_{\text{eff}} \leq 9000$  K. Even though a few of these stars have been classified previously as horizontal branch stars, to our knowledge, this is the first analysis with model spectra covering the range of surface gravities  $3.75 \leq \log g \leq 10$ . Of these sdAs, 1275 have estimated proper motions larger than 5 mas/yr, and 476 larger than 10 mas/yr. Because their spectra consists mainly of hydrogen lines, with cooler ones showing also Ca H&K, but no G- or CN-bands, we define their spectral types as sdA. We propose many of them are ELMs (Córscico & Althaus 2014a,b, 2015; Istrate et al. 2014a; Istrate, Tauris, & Langer 2014b; Istrate 2015) but until their binarity can be established (e.g. Gianninas et al. 2015), we classify only their spectral type.

#### 4.8 Noteworthy individual objects

Fig. 7 shows the spectrum of the AM CVn type ultra-compact double degenerate binary, SDSS J131954.47+591514.84, a new classification of a star with He-dominated atmosphere and He transfer. AM CVn objects are thought to be strong sources of gravitational waves (Nelemans 2005); however, only 43 such objects are known (Campbell et al. 2015; Levitan et al. 2015).

SDSS J141621.94+135224.20 (spectra with P-M-F 5458-56011-0636, Fig. 8) is a hot central star of a faint planetary nebula (CSPN) (PN G003.3+66.1) and was misclassified by Gentile Fusillo, Gänsicke, & Greiss (2015) as a cataclysmic variable. It is listed in the Southern H $\alpha$  Sky Survey

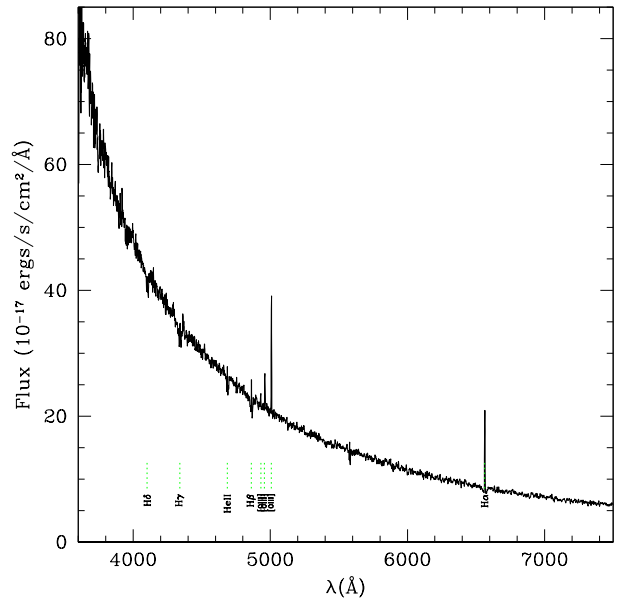


**Figure 8.** Spectra of the CSPN SDSS J141621.94+135224.20 ( $g = 18.202 \pm 0.019$ , proper motion = 12 mas/yr).

Atlas, however we could not detect any planetary nebula in either the SDSS image or WISE images. Thanks to its higher S/N, the new SDSS spectrum reveals the nebular emission lines of [OIII]  $\lambda\lambda$  4931, 4956, 5007 Å, which we have now identified for the first time in this star. The lack of He I absorption lines indicates that the central star is hotter than 70 kK. All photospheric absorption lines (H  $\delta$ , H  $\gamma$ , H  $\beta$ , H  $\alpha$  as well as HeII  $\lambda\lambda$  4686, 5412 Å) show central emissions. They are likely nebular lines, however a photospheric contribution cannot be excluded for very hot central stars.

SDSS J103455.90+240905.75 (P-M-F 6439-56358-0445) was classified by Girven et al. (2011) as DAB from spectra 2352-53770-0124, SDSS J100015.28+240724.60 (P-M-F 6459-56273-0598) was classified as DB from spectra 2344-53740-0137, and SDSS J101935.69+254103.04 (P-M-F 6465-56279-0808) was classified as DA from spectra 2349-53734-0523, but the new higher S/N spectra shows they are DOs.

Table 5 lists the columns of data provided in our electronic catalogue file, Table 6.

Table 7 lists 409 new classifications of stars already in Simbad (Strasbourg Astronomical Data Center), but for which new higher S/N spectra lead us to a different classification.

## 5 CONCLUSIONS AND DISCUSSION

We have identified 6 576 new white dwarf and subdwarf stars in the DR 12 of the SDSS, and estimated the masses for DAs and DBs, as well as the calcium contamination in DZs and carbon/helium abundances in DQs. We were able to extend our identifications down to  $T_{\text{eff}} = 5000$  K, although these are certainly not complete, as we relied also on proper motion measurements to distinguish between cool DCs and BL Lac objects. Proper motions are typically in-

**Table 5.** Columns provided in data table, Table 6.

Column No.	Heading	Description
1	Name	SDSS object name (SDSS 2000J+)
2	P-M-F	SDSS Plate number-Modified Julian date-Fiber
3	SN_g	SDSS g band signal to noise ratio
4	u_psf	SDSS u band PSF magnitude
5	u_err	SDSS u band uncertainty
6	g_psf	SDSS g band PSF magnitude
7	g_err	SDSS g band uncertainty
8	r_psf	SDSS r band PSF magnitude
9	r_err	SDSS r band uncertainty
10	i_psf	SDSS i band PSF magnitude
11	i_err	SDSS i band uncertainty
12	z_psf	SDSS z band PSF magnitude
13	z_err	SDSS z band uncertainty
14	E(B-V)	color excess
15	PM	USNO proper motion (mas yr <sup>-1</sup> )
16	l	galactic longitude (degrees)
17	b	galactic latitude (degrees)
18	T_eff	$T_{\text{eff}}$ (K)
19	T_err	$T_{\text{eff}}$ uncertainty (K)
20	log_g	$\log g$ (cgs)
21	log_gerr	$\log g$ uncertainty (cgs)
22	humanID	human classification
23	T_eff (3D)	$T_{\text{eff}}$ for pure DAs and DBs or $-\log(\text{Ca/He})$ for DZs or $-\log(\text{C/He})$ for DQs <sup>1</sup>
24	T_err (3D)	$T_{\text{eff}}$ uncertainty
25	log_g (3D)	$\log g$
26	log_gerr (3D)	$\log g$ uncertainty
27	Mass	calculated mass ( $M_{\odot}$ ), corrected to 3D-convection
28	Mass_err	mass uncertainty ( $M_{\odot}$ ), corrected to 3D-convection

complete below  $g \simeq 21$ . The resultant substantial increase in the number of spectroscopically confirmed white dwarfs is important because it allows the discovery of more rare objects like massive white dwarfs, magnetic white dwarfs, and He-dominated objects with oxygen lines. Extending the work of Kepler et al. (2007) and Rebassa-Mansergas et al. (2015), we find 94 white dwarf stars with masses above  $1 M_{\odot}$  and  $S/N \geq 15$ . Their volume corrected distribution is inhomogeneous which, if confirmed, indicates multiple formation processes, including mergers. The volume-limited sample of white dwarfs within 40 pc by Limoges, Bergeron, & Lépine (2015) finds 8% (22/288) of the local sample of white dwarfs have masses  $M > 1 M_{\odot}$ .

Massive white dwarfs are relevant both to the lower limit of core collapse SN and to white dwarf explosion or merger as SN Ia. Nomoto, Kobayashi, & Tominaga (2013) estimates that the observed <sup>64</sup>Zn abundances provides an upper limit to the occurrence of exploding O-Ne-Mg cores at approximately 20% of all core-collapse supernovae. The existence of different types of SN Ia indicates different types of progenitors do exist.

With our spectral model grid now extending from  $3.75 \leq \log g \leq 10$ , we identified 2675 stars with hydrogen dominated spectra, and surface gravities  $3 - 7\sigma$  larger than those of main sequence stars. Time-series spectroscopy is necessary to check if they are binaries, in order to establish what fraction of the sdA objects are ELM white dwarfs. If they were to have main sequence radii, their distances would be tens of kiloparsecs outside the disk due to their distance moduli of  $15 \leq m - M \leq 20$ . The substantial fraction of these stars that have measured proper motions, if at large distances, would also be runaway stars

or hypervelocity stars ( $v > 600$  km/s) (Brown 2015). The significant number of these stars probably indicates Population II formation lead to a considerable ratio of binary stars. De Rosa et al. (2014) determine that  $69 \pm 7\%$  of all A stars in the solar neighborhood are in binaries. The pre-white dwarf ages of low metallicity stars with main sequence masses  $0.9 M_{\odot}$  can amount to more than 8 Gyr, so white dwarfs originating from binary interactions of low mass, low metallicity stars should still be visible as extremely low mass white dwarfs. If the stars we classified as sdAs are in fact A-type main sequence stars, there is a large number of those at large distances from the galactic disk, and the galactic formation model would have to account for the continuous formation of low metallicity stars, perhaps from the continuous accretion of dwarf galaxies (Camargo et al. 2015; The DES Collaboration et al. 2015). Our analysis of their spatial distribution shows no concentrations.

## ACKNOWLEDGMENTS

S.O.K., I.P., G.O., A.D.R., and A.D.M.V. are supported by CNPq-Brazil. D.K. received support from programme Science without Borders, MCIT/MEC-Brazil. N.R. is supported by the German Aerospace Center (DLR, grant 05 OR 1507). This research has made use of NASA's Astrophysics Data System.

Funding for SDSS-III has been provided by the Alfred P. Sloan Foundation, the Participating Institutions, the National Science Foundation, and the U.S. Department of Energy Office of Science. The SDSS-III web site is <http://www.sdss3.org/>.

SDSS-III is managed by the Astrophysical Research Consortium for the Participating Institutions of the SDSS-III Collaboration including the University of Arizona, the Brazilian Participation Group, Brookhaven National Laboratory, Carnegie Mellon University, University of Florida, the French Participation Group, the German Participation Group, Harvard University, the Instituto de Astrofísica de Canarias, the Michigan State/Notre Dame/JINA Participation Group, Johns Hopkins University, Lawrence Berkeley National Laboratory, Max Planck Institute for Astrophysics, Max Planck Institute for Extraterrestrial Physics, New Mexico State University, New York University, Ohio State University, Pennsylvania State University, University of Portsmouth, Princeton University, the Spanish Participation Group, University of Tokyo, University of Utah, Vanderbilt University, University of Virginia, University of Washington, and Yale University.

## REFERENCES

- Abazajian, K., et al. 2003, *AJ*, 126, 2081  
 Abazajian, K. N., et al. 2009, *ApJS*, 182, 543  
 Adelman-McCarthy, J. K., et al. 2006, *ApJS*, 162, 38  
 Ahn C. P., et al., 2014, *ApJS*, 211, 17  
 Alam S., et al., 2015, *ApJS*, 219, 12  
 Althaus, L. G., García-Berro, E., Isern, J., & Córscico, A. H. 2005, *A&A*, 441, 689  
 Althaus, L. G., Panei, J. A., Romero, A. D., Rohrmann R. D., Córscico A. H., García-Berro E., Miller Bertolami M. M. 2009a, *A&A*, 502, 207  
 Althaus, L. G., Panei, J. A., Miller Bertolami, M. M., García-Berro E., Córscico A. H., Romero A. D., Kepler S.O., Rohrmann R. D. 2009b, *ApJ*, 704, 1605  
 Althaus L. G., Miller Bertolami M. M., Córscico A. H., 2013, *A&A*, 557, A19  
 Arnold R., Gilmore G., 1992, *MNRAS*, 257, 225  
 Bergeron P., Saffer R. A., Liebert J., 1992, *ApJ*, 394, 228  
 Bell K. J., Kepler S. O., Montgomery M. H., Hermes J. J., Harrold S. T., Winget D. E., 2015, *ASPC*, 493, 217  
 Bergeron P., et al., 2011, *ApJ*, 737, 28  
 Brown W. R., 2015, *ARA&A*, 53, 15  
 Brown W. R., Kilic M., Allende Prieto C., Kenyon S. J., 2010, *ApJ*, 723, 1072  
 Brown W. R., Kilic M., Allende Prieto C., Kenyon S. J., 2012, *ApJ*, 744, 142  
 Brown W. R., Kilic M., Allende Prieto C., Gianninas A., Kenyon S. J., 2013, *ApJ*, 769, 66  
 Bolton A. S., et al., 2012, *AJ*, 144, 144  
 Camargo D., Bica E., Bonatto C., Salerno G., 2015, *MNRAS*, 448, 1930  
 Campbell H. C., et al., 2015, *MNRAS*, 452, 1060  
 Córscico A. H., Althaus L. G., 2014, *ApJ*, 793, L17  
 Córscico A. H., Althaus L. G., 2014, *A&A*, 569, A106  
 Córscico A. H., Althaus L. G., 2015, *ASPC*, 493, 221  
 Dawson K. S., et al., 2013, *AJ*, 145, 10  
 De Rosa R. J., et al., 2014, *MNRAS*, 437, 1216  
 The DES Collaboration, et al., 2015, *arXiv*, arXiv:1508.03622  
 Doherty C. L., Gil-Pons P., Siess L., Lattanzio J. C., Lau H. H. B., 2015, *MNRAS*, 446, 2599.  
 Drake, A. J. et al., 2009, *ApJ*, 696, 870  
 Drake A. J., et al., 2012, in Griffin E., Hanisch R., Seaman R. eds, *Proc. IAU Symp. 285, New Horizons in Time-Domain Astronomy*. Cambridge Univ. Press, Cambridge, p. 306  
 Dreizler S., Schuh S. L., Deetjen J. L., Edelmann H., Heber U., 2002, *A&A*, 386, 249  
 Drilling J. S., Jeffery C. S., Heber U., Moehler S., Napiwotzki R., 2013, *A&A*, 551, A31  
 Dufour P., 2011, in Hoard D. W. ed., *White Dwarf Atmospheres and Circumstellar Environments*. Wiley, New York, p. 53  
 Dufour P., Liebert J., Fontaine G., Behara N., 2007, *Nature*, 450, 522  
 Dufour P., Vornanen T., Bergeron P., Fontaine B., A., 2013, in Krzesiński J, Stachowski G., Moskalik P.m Bajan K., eds., *ASP Conf. Ser. Vol. 469, 18th European White Dwarf Workshop*. Astron. Soc. Pac., San Francisco, p. 167  
 Eisenstein, D. J., et al. 2006, *ApJS*, 167, 40  
 Eisenstein D. J., et al., 2011, *AJ*, 142, 72  
 Falcon R. E., Winget D. E., Montgomery M. H., Williams K. A., 2010, *ApJ*, 712, 585  
 Falcon R. E., Winget D. E., Montgomery M. H., Williams K. A., 2012, *ApJ*, 757, 116  
 Farihi J., Gänsicke B. T., Koester D., 2013, *Sci*, 342, 218  
 Gänsicke B. T., Koester D., Girven J., Marsh T. R., Steeghs D., 2010, *Sci*, 327, 188  
 Genest-Beaulieu C., Bergeron P., 2014, *ApJ*, 796, 128  
 Gentile Fusillo N. P., Gänsicke B. T., Greiss S., 2015, *MNRAS*, 448, 2260  
 Gianninas A., Bergeron P., Fontaine G., 2005, *ApJ*, 631, 1100  
 Gianninas A., Bergeron P., Ruiz M. T., 2011, *ApJ*, 743, 138  
 Gianninas A., Dufour P., Kilic M., Brown W. R., Bergeron P., Hermes J. J., 2014, *ApJ*, 794, 35  
 Gianninas A., Kilic M., Brown W. R., Canton P., Kenyon S. J., 2015, *ApJ*, 812, 167  
 Girven J., Gänsicke B. T., Steeghs D., Koester D., 2011, *MNRAS*, 417, 1210  
 Graham J. R., Matthews K., Neugebauer G., Soifer B. T., 1990, *ApJ*, 357, 216  
 Green R. F., 1980, *ApJ*, 238, 685  
 Harris H. C., et al., 2003, *AJ*, 126, 1023  
 Heiter U., Jofré P., Gustafsson B., Korn A. J., Soubiran C., Thévenin F., 2015, *A&A*, 582, A49  
 Hermes J. J., Montgomery M. H., Winget D. E., Brown W. R., Kilic M., Kenyon S. J., 2012, *ApJ*, 750, L28  
 Hermes J. J., et al., 2013b, *MNRAS*, 436, 3573  
 Hermes J. J., et al., 2013a, *ApJ*, 765, 102  
 Hollands M. A., Gänsicke B. T., Koester D., 2015, *MNRAS*, 450, 681  
 Ibeling D., Heger A., 2013, *ApJ*, 765, L43  
 Istrate A. G., Tauris T. M., Langer N., Antoniadis J., 2014, *A&A*, 571, L3  
 Istrate A. G., Tauris T. M., Langer N., 2014, *A&A*, 571, A45  
 Istrate A. G., 2015, *ASPC*, 493, 487  
 Jura M., 2003, *ApJ*, 584, L91  
 Kawka A., Vennes S., 2014, *MNRAS*, 439, L90  
 Kepler S. O., Kleinman S. J., Nitta A., Koester D., Castanheira B. G., Giovannini O., Costa A. F. M., Althaus L., 2007, *MNRAS*, 375, 1315  
 Kepler S. O., et al., 2013, *MNRAS*, 429, 2934  
 Kepler S. O., et al., 2015, *MNRAS*, 446, 4078  
 Kilic M., Stanek K. Z., Pinsonneault M. H., 2007, *ApJ*, 671, 761  
 Kilic M., Brown W. R., Allende Prieto C., Agüeros M. A., Heinke C., Kenyon S. J., 2011, *ApJ*, 727, 3  
 Kilic M., Brown W. R., Allende Prieto C., Kenyon S. J., Heinke C. O., Agüeros M. A., Kleinman S. J., 2012, *ApJ*, 751, 141  
 Kleinman S. J., et al. 2004, *ApJ*, 607, 426  
 Kleinman S. J., Kepler S.O., Koester D., Pelisoli I., Peçanha V., Nitta A., Costa J.E.S., Krzesiński J., et al. 2013, *ApJS*, 204, 5.  
 Koester D., Kepler, S.O., 2015, *A&A*, in press.  
 Koester D., Weidemann V., Zeidler E.-M., 1982, *A&A*, 116, 147  
 Koester D., Knist S., 2006, *A&A*, 454, 951  
 Koester D., 2010, *Mem. Soc. Astron. Ital.*, 81, 921

- Koester D., Girven J., Gänsicke B. T., Dufour P., 2011, *A&A*, 530, A114
- Koester D., Gänsicke B. T., Farihi J., 2014, *A&A*, 566, A34
- Külebi B., Jordan S., Euchner F., Gänsicke B. T., Hirsch H. 2009, *A&A*, 506, 1341
- Lam M. C., Rowell N., Hambly N. C., 2015, *MNRAS*, 450, 4098
- Lépine S., Shara M. M., 2005, *ApJ*, 129, 1483
- Levitan D., Groot P. J., Prince T. A., Kulkarni S. R., Laher R., Ofek E. O., Sesar B., Surace J., 2015, *MNRAS*, 446, 391
- Li L., Zhang F., Han Q., Kong X., Gong X., 2014, *MNRAS*, 445, 1331
- Liebert J., Bergeron P., Holberg J. B., 2003, *AJ*, 125, 348
- Liebert J., et al., 2003, *AJ*, 126, 2521
- Liebert J., Bergeron P., Holberg J. B., 2005, *ApJS*, 156, 47
- Limoges M.-M. & Bergeron P. 2010, *ApJ*, 714, 1037
- Limoges M.-M., Bergeron P., Lépine S., 2015, *ApJS*, 219, 19
- Liu C., Li L., Zhang F., Zhang Y., Jiang D., Liu J., 2012, *MNRAS*, 424, 1841
- Marsh T. R., Dhillon V. S., Duck S. R., 1995, *MNRAS*, 275, 828
- Maxted P. F. L., Marsh T. R., Moran C. K. J., 2000, *MNRAS*, 319, 305
- Maxted P. F. L., et al., 2014a, *MNRAS*, 437, 1681
- Maxted P. F. L., Serenelli A. M., Marsh T. R., Catalán S., Mah-tani D. P., Dhillon V. S., 2014b, *MNRAS*, 444, 208
- Moehler S. & Bono G., 2008, arXiv:0806.4456v3
- Monet D. G., et al., 2003, *AJ*, 125, 984
- Munn J. A., et al., 2014, *AJ*, 148, 132
- Napiwotzki, R., 2007, in *ASP Conf. Ser. 372*, 15th European Workshop on White Dwarfs, ed. R. Napiwotzki & M. R. Burleigh (San Francisco, CA: ASP), 387
- Nelemans G., 2005, in *Hameury J.M., Lasota J.-P., Astron. Soc. Pac. Conference Series Vol. 330*, The Astrophysics of Cataclysmic Variables and Related Objects, p. 27
- Németh P., Kawka A., Vennes S., 2012, *MNRAS*, 427, 2180
- Nemeth P., Östensen R., Vos J., Kawka A., Vennes S., 2014a, in van Grootel V., Green E., Fontaine G., Charpinet S., eds. *ASP Conf. Ser. Vol. 481*, 6th Meeting on Hot Subdwarf Stars and Related Objects. Astron. Soc. Pac., San Francisco, p. 75
- Nemeth P., Östensen R., Tremblay P., Hubeny I., 2014b, in van Grootel V., Green E., Fontaine G., Charpinet S., eds. *ASP Conf. Ser. Vol. 481*, 6th Meeting on Hot Subdwarf Stars and Related Objects. Astron. Soc. Pac., San Francisco, p. 95
- Nomoto K., Kobayashi C., Tominaga N., 2013, *ARA&A*, 51, 457
- Pelletier C., Fontaine G., Wesemael F., Michaud G., Wegner G., 1986, *ApJ*, 307, 242
- Napiwotzki R., 1997, *A&A*, 322, 256
- Nomoto K., 1984, *ApJ*, 277, 791
- Nomoto K., 2014, *IAUS*, 296, 27
- Raddi R., Gänsicke B. T., Koester D., Farihi J., Hermes J. J., Scaringi S., Breedt E., Girven J., 2015, *MNRAS*, 450, 2083
- Rauch T., Rudkowski A., Kampka D., Werner K., Kruk J. W., Moehler S., 2014, *A&A*, 566, A3
- Rebassa-Mansergas A., Gänsicke B. T., Rodríguez-Gil P., Schreiber M. R., Koester D., 2007, *MNRAS*, 382, 1377
- Rebassa-Mansergas A., Agurto-Gangas C., Schreiber M. R., Gänsicke B. T., Koester D., 2013, *MNRAS*, 433, 3398
- Rebassa-Mansergas A., Rybicka M., Liu X.-M., Han Z., García-Berro, E. 2015, *MNRAS*, in press.
- Reindl N., Rauch T., Werner K., Kepler S. O., Gänsicke B. T. & Gentile Fusillo N. P. 2014, *A&A*, preprint (arXiv1410.7666)
- Renedo I., Althaus L. G., Miller Bertolami M. M., Romero A. D., Córscico A. H., Rohrmann R. D., García-Berro E. 2010, *ApJ*, 717, 183
- Romero A. D., Córscico A. H., Althaus L. G., Kepler S. O., Castanheira B. G., Miller Bertolami M. M., 2012, *MNRAS*, 420, 1462
- Romero A. D., Campos F., Kepler S. O., 2015, *MNRAS*, 450, 3708
- Schimeczek C., Boblest S., Meyer D., Wunner G., 2013, *PhRvA*, 88, 012509
- Schimeczek C., Wunner G., 2014a, *CoPhC*, 185, 614
- Schimeczek C., Wunner G., 2014b, *ApJS*, 212, 26
- Schmidt M., 1968, *ApJ*, 151, 393
- Schmidt M., 1975, *ApJ*, 202, 22
- Smartt S. J., 2009, *ARA&A*, 47, 63
- Smartt S. J., Eldridge J. J., Crockett R. M., Maund J. R., 2009, *MNRAS*, 395, 1409
- Smee S. A., et al., 2013, *AJ*, 146, 32
- Stobie R. S., Ishida K., Peacock J. A., 1989, *MNRAS*, 238, 709
- Straniero O., Domínguez I., Imbriani G., Piersanti L., 2003, *ApJ*, 583, 878
- Tremblay P.-E., Ludwig H.-G., Steffen M., Freytag B., 2013, *A&A*, 559, A104
- Tremblay P.-E., Kalirai J. S., Soderblom D. R., Cignoni M., Cummings J., 2014, *ApJ*, 791, 92
- Van Grootel V., Fontaine G., Brassard P., Dupret M.-A., 2013, *ApJ*, 762, 57
- Valenti S., et al., 2009, *Nature*, 459, 674
- Werner K., Rauch T., Kepler S. O., 2014, *A&A*, 564, A53
- Winget D. E. et al., 1987, *ApJ*, 315, L77–L81
- Woosley S. E., Heger A., 2015, *ApJ*, 810, 34

**Table 6.** New White Dwarf Stars. Notes: P-M-F are the Plate-Modified Julian Date-Fiber number that designates an SDSS spectrum. A : designates an uncertain classification. The columns are fully explained in Table 5. When  $\sigma(\log g) = 0.000$ , we have assumed  $\log g = 8.0$ , not fitted the surface gravity. The full table is available online, and at <http://astro.if.ufrgs.br/keplerDR12.html>.

#SDSSJ	P-M-F	S/N	u	su	g	sg	r	sr	i	si	z	sz	E(B-V)	ppm	long	lat	sp	Teff	sT	logg	slogg	Teff	dTeff	logg	dlogg	mass	dmass	
#		(mag)	(mag)	0.001"	(o)	(o)		(K)	(K)	(cgs)	(cgs)	(K)	(K)	(cgs)	(cgs)	(Msun)	(Msun)											
000000.46+174808.91	6207-56239-0156	005	21.460	0.125	20.966	0.033	20.992	0.045	21.063	0.068	21.211	0.322	0.028	0.028	024.4	106.0	-43.4	DA	09683	00132	7.945	0.174	09635	0132	7.680	0.170	0.459	0.067
000007.84+304606.35	7134-56566-0587	011	20.208	0.039	19.665	0.017	19.534	0.021	19.495	0.023	19.562	0.059	0.060	44.69	110.1	-30.8	DA:	07545	00064	7.616	0.117	07566	0064	7.470	0.120	0.366	0.042	
000013.17-102750.57	7167-56604-0281	006	21.356	0.146	20.583	0.035	20.548	0.039	20.556	0.053	20.940	0.310	0.050	07.58	084.6	-69.4	sdA:	07836	00119	5.520	0.376							
000035.88-024622.11	4354-55810-0305	011	20.979	0.081	19.803	0.019	19.666	0.027	19.650	0.023	19.591	0.063	0.037	007.5	094.2	-62.8	sdA	07893	00065	6.143	0.189	07893	0065	5.940	0.190	0.153	0.0016	
000043.52+351644.26	7145-56567-0818	006	21.132	0.112	20.585	0.030	20.531	0.040	20.534	0.051	20.477	0.175	0.071	015.3	111.4	-26.5	DA	09208	00104	8.095	0.149	09178	0104	7.820	0.150	0.521	0.064	
000049.03-105805.58	7167-56604-0202	010	20.992	0.104	20.036	0.032	19.768	0.027	19.774	0.032	19.717	0.116	0.036	002.0	084.1	-69.9	sdA	07092	00083	6.180	0.259	07117	0083	6.003	0.260	0.149	0.0040	
000052.60+265459.66	6511-56540-0042	017	19.480	0.044	18.577	0.022	18.258	0.015	18.174	0.017	18.129	0.028	0.046	005.7	109.2	-34.6	sdA	06862	00045	5.963	0.155	06889	0045	5.804	0.150	0.147	0.0009	
000100.52-100222.12	7167-56604-0234	005	21.850	0.308	20.956	0.088	20.953	0.071	21.108	0.094	21.952	0.858	0.036	000.0	085.7	-69.2	DA	08977	00131	8.292	0.164	08969	0131	8.020	0.160	0.609	0.088	
000110.91+285342.93	7134-56566-0368	004	21.433	0.116	21.032	0.041	20.916	0.045	20.958	0.069	20.535	0.172	0.068	00.00	109.9	-32.7	DA:	07722	00166	8.229	0.236	07735	0166	8.090	0.240	0.646	0.135	
000133.32+170237.76	6173-56238-0428	005	21.173	0.121	20.752	0.038	20.974	0.059	21.087	0.078	22.163	0.567	0.028	000.0	106.2	-44.2	DA	11198	01000	7.690	0.500	11283	1000	7.540	0.500	0.409	0.176	
000134.78+201514.44	6170-56240-0638	009	20.626	0.080	20.232	0.024	20.126	0.028	20.053	0.037	20.048	0.147	0.073	56.89	107.3	-41.1	DA	07512	00093	8.343	0.132	07520	0093	8.230	0.130	0.726	0.080	
000134.86+321616.24	6498-56565-0910	009	20.541	0.059	20.204	0.025	20.184	0.035	20.428	0.062	20.858	0.314	0.051	000.0	110.8	-29.4	DA	10088	00089	8.189	0.094	10042	0089	7.920	0.090	0.558	0.041	

**Table 7.** New Classification of Known White Dwarf Stars.

#SDSSJ	P-M-F	S/N	u	su	g	sg	r	sr	i	si	z	sz	E(B-V)	ppm	long	lat	sp	Teff	sT	logg	slogg	Teff	dTeff	logg	dlogg	mass	dmass	
#		(mag)	(mag)	0.001"	(o)	(o)		(K)	(K)	(cgs)	(cgs)	(K)	(K)	(cgs)	(cgs)	(Msun)	(Msun)											
000054.40-090806.92	7167-56604-0806	022	19.317	0.042	18.997	0.033	18.952	0.019	19.030	0.029	19.094	0.061	0.050	53.63	087.0	-68.4	DQ	07957	01000	8.000	0.000	-log(C/He)=8.000	0.000					
000307.06+241211.68	6879-56539-0704	064	16.159	0.022	16.190	0.022	16.556	0.028	16.806	0.017	17.053	0.026	0.147	04.41	109.0	-37.4	sdB	28566	00099	5.503	0.017							
000309.26-060233.49	7147-56574-0956	007	20.571	0.058	20.065	0.021	19.970	0.020	19.966	0.027	19.926	0.074	0.041	054.6	092.2	-66.0	DA	08264	00097	7.157	0.218	08259	0097	6.940	0.220	0.234	0.039	
000309.26-060233.49	7148-56591-0586	008	20.571	0.058	20.065	0.021	19.970	0.020	19.966	0.027	19.926	0.074	0.041	054.6	092.2	-66.0	DA	08489	00099	8.164	0.162	08500	0099	7.930	0.160	0.559	0.076	
000321.60-015310.86	4365-55539-0502	015	19.232	0.028	19.216	0.027	19.294	0.020	19.498	0.025	19.728	0.072	0.041	053.8	096.4	-62.3	DA	06126	00103	9.320	0.214	06110	0103	9.370	0.210	1.285	0.072	